

Measurement of atmospheric transparencies with LIDAR for Telescope Array

T.Tomida*, Y.Tsuyuguchi*, H.Ukai*, K.Honda*, M.Chikawa†, S.Udo‡,
G.B.Thomson§ and M.Fukushima¶ for the Telescope Array Collaboration

*University of Yamanashi, Kofu, Yamanashi, 400-8511, Japan

†Department of Physics, Kinki University, Higashi-Osaka, 577-8502, Japan

‡Kanagawa University, Yokohama, Kanagawa, 221-8686, Japan

§Rutgers University, 136 Frelinghuysen Road, Piscataway, NJ 08854, USA

¶Institute for Cosmic Ray Research, The University of Tokyo, Kashiwa, Chiba, 277-8582, Japan

Abstract. Atmospheric monitoring is important for estimating the energy of cosmic rays and determining the detector aperture for experiments using the air fluorescence technique. Since September 2007, we have been measuring the daily variation of atmospheric transparencies using a new data acquisition system of the LIDAR constructed for the TA experiment. The measurements are performed before and after air fluorescence observations. The vertical and horizontal laser shots enable us to calculate the extinction coefficients at the surface and above 1~3 km from the ground. In this paper, we describe the LIDAR system, the analysis method and results on the extinction coefficient.

Keywords: UHECRs, Atmospheric monitoring, LIDAR

I. INTRODUCTION

Atmospheric monitoring is important for estimating the energy of cosmic rays and determining the detector aperture for experiments using the air fluorescence technique. In order to correct detection atmospheric fluorescence light induced by an air shower which corresponds to primary cosmic ray energy, the atmospheric transparency have been measured using two kinds of laser system in Telescope Array (TA). One laser system is called LIDAR (LIght Detection And Ranging) which observes back scattered light of laser by air molecules (Rayleigh scattering) and by aerosols (Mie scattering) in the atmosphere.

LIDAR method is widely used in the ground based observations of aerosols. The other laser system is located at the middle of three fluorescence detector (FD) stations, the scattering light in a atmosphere are observed by three fluorescence detector stations. This system is called CLF (Center Laser Facility).

II. THE LIDAR SYSTEM AND OBSERVATION

The LIDAR system had been installed in the dome at Black Rock Mesa (BRM) in the TA site from 2005 [1] [2]. This system is located 100 m apart from the fluorescence detector (FD) station. YAG laser shot a 355 nm wavelength light of maximum energy with 4 mJ

by 1 Hz. The backscattering light is received by 30 cm diameter telescope including a PMT with a UV filter. The laser and the optical system are mounted on the steerable telescope. The signals detected by the PMT are recorded with the digital oscilloscope, digitized data are transferred to a Linux PC. The dome and LIDAR system are controlled by Linux PC in the dome which is connected to a PC in the FD station via the network. The observation using LIDAR system is able to operate from FD station.

Since September 2007, we have been measuring the daily variation of atmospheric transparencies using a new data acquisition system of the LIDAR. The measurements of atmospheric condition are performed before and after air fluorescence observations. In order to obtain the extinction coefficients (α) at the surface, 500 shots of laser are shot to northward horizontal way with high and low energy respectively. Also, 500 vertical laser shots are shot with same energies of horizontal shots. The measurement time of 4 kinds shots is about 40 minutes.

III. DATA ANALYSIS

We have analyzed about 300 measurements from Sep. 2007 to Nov. 2008. The extinction coefficients (α) at the surface are determined by solving the slope method [3] [4] only using high energy shots data, because the coverage of the slope method for low energy shots is too short length to an analysis. The vertical α are determined by solving the Klett's method [5] which is included boundary condition that α at high altitude is same one calculated from only considering pure Rayleigh scattering.

Example of the α at each height from ground is shown in Fig. 1. Fig. 1(a) shows the result calculated from vertical shot data with high energy shot (thick blue line) and low energy shot (thick green line). When low energy data of vertical shots are sometime unstable because the intensity of back scattering light is too small, α are calculated only from high energy data as shown in Fig. 1(b). In these figures, thick red line above 8 km means data beyond the observation limit, the height of changing from thick blue line to thick red line means

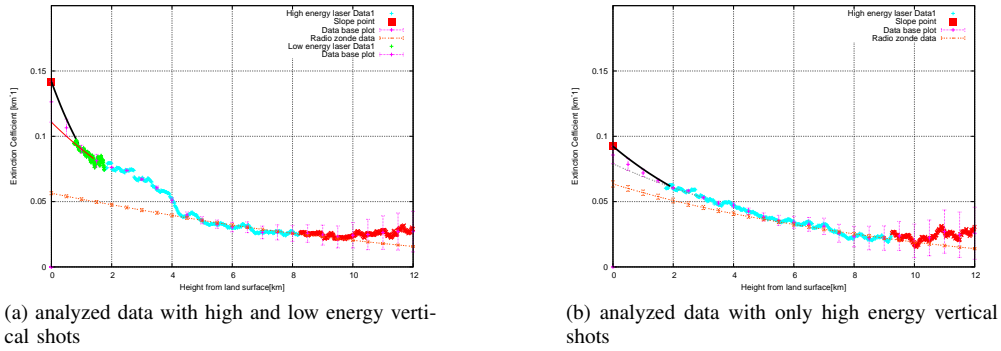


Fig. 1. The extinction coefficient as a function of height from the surface.

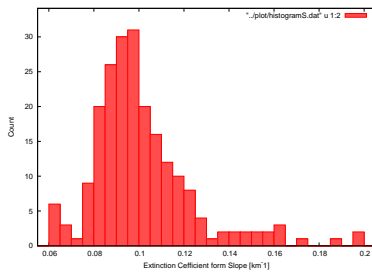


Fig. 2. Distribution of the horizontal extinction coefficient.

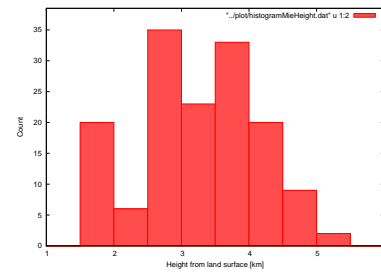


Fig. 3. Distribution of the maximum height at which the aerosol contribution is measureable.

the height of the boundary condition in Klett's method. In these figures, red square at 0 km shows α calculated by the slope method using horizontal high energy shots. The red dot line in lower part of these figures shows α of pure Rayleigh scattering calculated from Radiosonde data observed at Elko (Nevada) where 340 km apart from the TA site. α at near surface less than about 1 km or 2 km couldn't be obtained with the present observation method. Therefore, we have estimated α in this height region with two kind methods. One is shown with thick black line in the figure which is connected with the exponential curve between α at 0 km obtained by the slope method and observed α at lowest height. The other estimated value is shown with red line and gray dot line which are extrapolated with the exponential curve for α of about 1 km range obtained with Klett's method.

We have classified observed data into four kinds depending on the characteristics of atmospheric and experimental condition. The number of events with nice atmospheric condition without clouds and large scattering matter, we call "flag0", is about 150. The atmospheric condition of "flag1" event is included with scattering matter, the number of events of "flag1" is about 50. We report the characteristics of α for "flag0" and "flag1" which amount to 200 events.

The distribution of $\alpha_{0\text{km}}$ at the surface obtained from horizontal shots is shown in Fig. 2. The average of $\alpha_{0\text{km}}$ is $0.11 \text{ [km}^{-1}\text{]}$. A lot of events are included with $\alpha_{0\text{km}}$ between $0.08 \sim 0.12 \text{ [km}^{-1}\text{]}$. The value of $\alpha_{0\text{km}}$ obtained from our measurement may be reasonable by taking account of the fact that $\alpha_{0\text{km}}$ (Rayleigh scattering)

is about $0.06 \text{ [km}^{-1}\text{]}$.

α (Mie scattering) is calculated to subtract α (Rayleigh scattering) from α (measurement). The maximum height at which the aerosol contribution is measureable is researched with 500 m resolution considering 1.5σ of α (measurement) as shown in Fig. 3. A lot of event distribute between 2.5 km and 4.5 km.

Two examples of the distribution of α (Mie scattering) are shown with red line in Fig. 4(a) and Fig. 4(b). Since the distribution of aerosol is usually exponential, one characterize it as $\exp(-h/h_0)$, where h is the height from the surface and h_0 is called "scale height" of the aerosol distribution. We assume the distribution of α (Mie scattering) is explained by same function of $\exp(-h/h_0)$. The green dot line in these figures show a function as $\alpha_{0\text{km}}$ (Mie scattering) $\times \exp(-h/h_0)$, where h_0 is 1.2 km. Fig. 4(a) is an example of similar distribution while Fig. 4(b) is an example of slightly different distribution.

The Vertical Aerosol Optical Depth (VAOD) is calculated easily to integrate the α (Mie scattering) distribution from the surface as shown in Fig. 4. For searching the confidential VAOD, 91 events measured α less than about 2 km height are selected from "flag0" and "flag1" events. The examples VAOD as a function of height are shown in Fig. 5(a) and Fig. 5(b). Red line and green dot line in these figures indicate VAOD calculated using $\alpha_{0\text{km}}$ (Mie scattering) and α estimated from Klett's method data respectively. Blue dot line indicates VAOD calculated from function as $\alpha_{0\text{km}}$ (Mie scattering) $\times \exp(-h/(1.2 \text{ km}))$ which is shown with green dot line

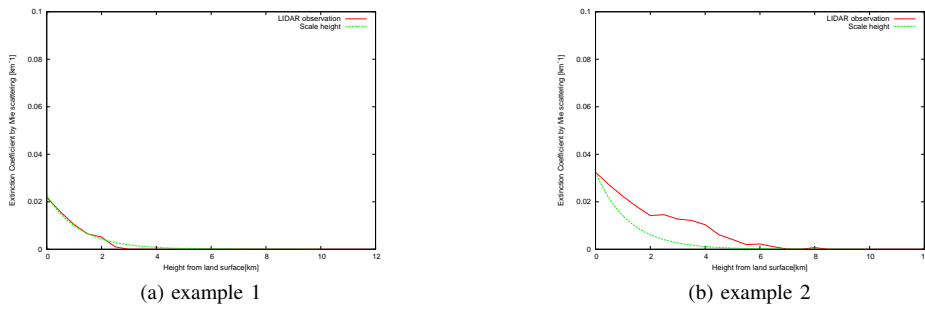


Fig. 4. The extinction coefficient of Mie scattering calculated scale height and LIDAR observation respectively.

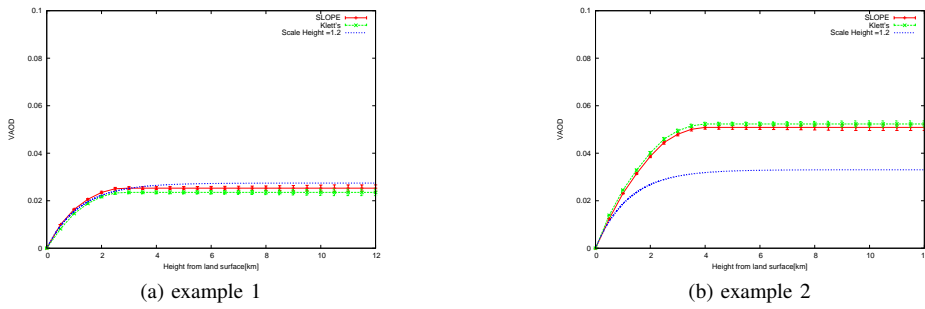


Fig. 5. VAOD calculated scale height and LIDAR observation respectively.

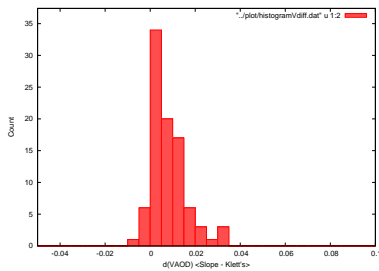


Fig. 6. Distribution of VAOD of difference between estimation from the slope and Klett's method.

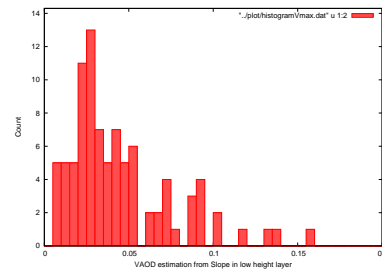


Fig. 7. Distribution of VAOD estimation from the Slope method in low height layer.

in Fig. 4. For the example of Fig. 5(a), three values of VAOD are similar distributions. Other example as shown in Fig. 5(b) indicate that both VAOD distributions obtained by the measurement are similar one except the distribution calculated from the scale height equation.

The distribution of the difference VAOD calculated using α_{0km} (Mie scattering) and α estimated from Klett's method data is shown in Fig. 6. The difference of almost events is less than 0.02 for selected 91 events. It means that VAOD of selected events is reliable value.

The distribution of VAOD for selected events is shown in Fig. 7. VAOD of 76% is less value than 0.055, VAOD of 24% is distributed between 0.06 and 0.16 from this distribution.

IV. CENTRAL LASER FACILITY

The Central Laser Facility (CLF) uses also a YAG laser as the test beam for FDs. A 355 nm is close color to second prominent wavelength 357 nm of the

fluorescence light generated by air shower particles. Furthermore, we are expecting that the amount of scattered light from emitted 5 mJ laser at a height of 2 km is roughly equal to the fluorescence light generated by 10^{20} eV cosmic ray.

At the CLF site, 20' container box is established and each components of optics, control PCs and devices are contained into the box [6]. The CLF contains a weather monitor and an LPG generator system in addition to main components, these systems are working autonomously. When it is raining during the operation, the rain sensor of weather monitor makes a warning and restrains the control PC from the laser shooting at that time. If the temperature becomes below 10°C, the generator control PC starts the generator to switch the heater on. (LPG generator is not working excepting the laser operating time and the heater required condition)

The operation of CLF is performed every 30 minutes during the FD observation. 100 shots of laser are shoot

with 10 Hz, shot time is being controlled by the “GPSy II” GPS capture module [7]. This precise information is useful for trigger timing calibration between FDs. Before each operation, laser energy is measured for energy calibration and linearity check. For this purpose, two energy probes are installed on the beam path inside of container. These two probes measure the laser energy directly and relatively, so we can estimate the energy of emitted laser using the ratio between two probes.

The CLF operation is been continuing since Dec. 2008. Laser tracks are detected by the FD telescopes and recorded to the system in the same way as the air shower tracks. Fig. 8 shows the example images of the CLF laser track. When some clouds cover above the CLF, the track

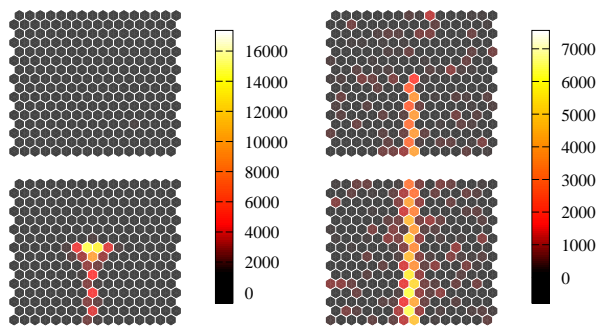


Fig. 8. Images of CLF laser track. On left panel, the laser is stopped at middle of the lower view because of the cloud. Right image was acquired at clear night. Color bars are showing ADC counts.

appears only in the lower view. However, those images as shown in a left panel help us to roughly estimate the height of cloud’s bottom. It can be considered as the part of cloud monitoring system which supports the IR camera [8] installed at BRM-FD station.

Detected photon intensity as function of height is shown in Fig. 9. In this figure, about 30 waveform of laser shots had been summed. Error bars based on the standard deviation of those waveforms are small enough, and the significant bumps which can be found especially in upper view signal are caused by the gaps between adjacent PMTs. The shapes of bumps are reflecting the difference between two stations (BRM and LR : LongRidge) about the positions where laser tracks are projected onto.

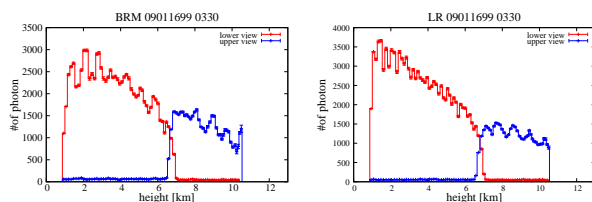


Fig. 9. Number of photon according to height from the ground. Red line shows signals of the lower view and blue line shows those of upper view in both of BRM (left) and LR (right).

In the analysis of CLF, the difference between a

simulated photon intensity without aerosols and an actual one represents the absorption caused by the atmospheric aerosols. Using some approximation and the ratio of photon intensities, the VAOD which expresses the integration of extinction coefficient α by height is obtained. (See [9] for the detailed determination of VAOD.) Supply of the information about atmospheric condition on every 30 min. would help us to calibrate the energy scale and to calculate the acceptance of FDs.

ACKNOWLEDGEMENTS

The Telescope Array experiment is supported by the Ministry of Education, Culture, Sports, Science and Technology-Japan through Kakenhi grants on priority area (431) “Highest Energy Cosmic Rays”, basic researches 18204020(A), 18403004(B) and 20340057(B); by the U.S. National Science Foundation awards PHY-0601915, PHY0703893, PHY-0758342, and PHY-0848320 (Utah) and PHY-0305516 (Rutgers); by the Korean Science and Engineering Foundation (KOSEF, Grant No. R01-2007-000-21088-0); by the Russian Academy of Sciences, RFBR grants 07-02-00820a and 09-07-00388a (INR), the FNRS contract 1.5.335.08, IISN and Belgian Science Policy under IUAP VI/11 (ULB). The foundations of Dr. Ezekiel R. and Edna Wattis Dumke, Willard L. Eccles and the George S. and Dolores Dore Eccles all helped with generous donations. The State of Utah supported the project through its Economic Development Board, and the University of Utah through the Office of the Vice President for Research. The experimental site became available through the cooperation of the Utah School and Institutional Trust Lands Administration (SITLA), U.S. Bureau of Land Management and the U.S. Air Force. We also wish to thank the people and the officials of Millard County, Utah, for their steadfast and warm support. We gratefully acknowledge the contributions from the technical staffs of our home institutions.

REFERENCES

- [1] Chikawa, M. et al., *Atmospheric Monitoring with LIDAR method for the TA Experiment*, Proc. 29th Int. Cosmic-Ray Conference
- [2] Chikawa, M. et al., *The Atmospheric Monitoring with a LIDAR and an Infra-red Camera at Black Rock Measa in the Utah desert*, Proc. 30th Int. Cosmic-Ray Conference, (**HE 1.5**), pages 1025-1028, 2007
- [3] R.T.H.Collis, *Lidar: a new atmospheric probe*, Quart. J. Roy. Meteorol. Soc. **92**, p. 220, 1966
- [4] W.Viezee, et al., *Lidar observations of airfield approach conditions; An exploratory study*, J. App. Meteorol. **8**, p.274, 1969
- [5] J.D.Klett, *Stable analytical inversion solution for processing lidar retrms*, Appl. Opt. **24**, 1609-1613, 1985
- [6] Udo, S. et al., *The Central Laser Facility at the Telescope Array*, Proc. 30th Int. Cosmic-Ray Conference, Vol.5 (**HE.2**), pages 1021-1024, 2007
- [7] Smith, J. D. et al., *GPSY2: A programmable hardware module for precise absolute time event generation and measurement*, Proc. 30th Int. Cosmic-Ray Conference, Vol.5 (**HE.2**), pages 997-1000, 2007
- [8] Chikawa, M. et al., *Cloud Monitoring with an Infra-Red Camera for the Telescope*, In this Conference
- [9] Abbasi, R. et al., *Techniques for measuring atmospheric aerosols at the high resolution fly’s eye experiment*, Astroparticle Physics, **25**, 74-83, 2006